

Photon pair source based on parametric fluorescence in periodically poled twin-hole silica fiber

**Kien Phan Huy, Anh Tuan Nguyen, Edouard Brainis,
Marc Haelterman, and Philippe Emplit**

*Service d'Optique et Acoustique, Université Libre de Bruxelles (U.L.B.),
Avenue F.D. Roosevelt 50, CP 194/5, 1050 Bruxelles, Belgium*
kphanhuy@ulb.ac.be

**Costantino Corbari, Albert Canagasabay, Morten Ibsen and Peter G.
Kazansky**

*Optoelectronics Research Centre, University of Southampton,
Southampton Hampshire SO17 1BJ, United Kingdom*

Olivier Deparis*, Andrei A. Fotiadi, and Patrice Mégret

*Service d'Electromagnétisme et de Télécommunications,
Faculté Polytechnique de Mons, 31 boulevard Dolez, B-7000 Mons, Belgium*

Serge Massar

*Laboratoire d'Information Quantique, CP 225, Université Libre de
Bruxelles (U.L.B.), Boulevard du Triomphe, 1050 Bruxelles, Belgium*
smassar@ulb.ac.be

Abstract: We present observations of quasi-phase matched parametric fluorescence in a periodically poled twin-hole silica fiber. The phase matching condition in the fiber enables the generation of a degenerate signal field in the fiber-optic communication band centered on 1556 nm. We performed coincidence measurements and a Hong-Ou-Mandel experiment to validate that the signal arises from photon pairs. A coincidence peak with a signal to noise ratio (SNR) of 4 using 43 mW of pump power and a Hong-Ou-Mandel dip showing 40% net visibility were measured. Moreover, the experiments were performed with standard single mode fibers spliced at both ends of the poled section, which makes this source easy to integrate in fiber-optic quantum communication applications.

© 2007 Optical Society of America

OCIS codes: (000.1600) Classical and Quantum Physics; (060.4370) Nonlinear Optics, fibers; (190.2620) Frequency conversion; (190.4410) Nonlinear optics, parametric processes.

References and links

1. A. K. Ekert, "Quantum cryptography based on Bells theorem," *Phys. Rev. Lett.* **67**, 661–663 (1991).
2. A. K. Ekert, J. G. Rarity, P. R. Tapster, and G. M. Palma, "Practical quantum cryptography based on two-photon interferometry," *Phys. Rev. Lett.* **69**, 1293–1295 (1992).
3. T. Jennewein, C. Simon, G. Weihs, H. Weinfurter, and A. Zeilinger, "Quantum Cryptography with Entangled Photons," *Phys. Rev. Lett.* **84**, 4729–4732 (2000).
4. W. Tittel, J. Brendel, H. Zbinden, and N. Gisin, "Quantum Cryptography Using Entangled Photons in Energy-Time Bell States," *Phys. Rev. Lett.* **84**, 4737–4740 (2000).

5. S. Tanzilli, H. De Riedmatten, W. Tittel, H. Zbinden, P. Baldi, M. De Micheli, D. B. Ostrowsky and N. Gisin, "Highly efficient photon-pair source using periodically poled lithium niobate waveguide," *Electron. Lett.* **37**, 26–28 (2001).
6. M. Fiorentino, P. L. Voss, J. E. Sharping and P. Kumar, "All-fiber photon-pair source for quantum communications," *IEEE Photon. Technol. Lett.* **14**, 983–985 (2002).
7. J. Rarity, J. Fulconis, J. Duligall, W. Wadsworth, and P. Russell, "Photonic crystal fiber source of correlated photon pairs," *Opt. Express* **13**, 534–544 (2005), <http://www.opticsexpress.org/abstract.cfm?id=82392>.
8. G. Bonfrate, V. Pruneri, P. G. Kazansky, P. Tapster and J. G. Rarity, "Parametric fluorescence in periodically poled silica fibers," *Appl. Phys. Lett.* **75**, 2356–2358 (1999).
9. C. Corbari, A. Canagasabay, M. Ibsen, F. P. Mezzapesa, C. Codemard, J. Nilsson and P. G. Kazansky, "All-fibre frequency conversion in long periodically poled silica fibres," in *Optical Fiber Communication Conference, 2005, Technical Digest, Anheim 5-11 March 2005 OFB3*.
10. R. A. Myers, N. Mukherjee, and S. R. J. Brueck, "Large second-order nonlinearity in poled fused silica," *Opt. Lett.* **16**, 1732–1734 (1991).
11. A. Fotiadi, O. Deparis, P. M egret, C. Corbari, A. Canagasabay, M. Ibsen, and P. G. Kazansky, "All fiber frequency doubled Er/Brillouin laser," in *CLEO/QELS 2006 Long Beach 21-26 May 2006 CTuI3*.
12. P. Merritt, R. P. Tatam, and D. A. Jackson, "Interferometric chromatic dispersion measurements on short length-*sof* monomode optical fiber," *J. Lightwave Technol.* **7**, 703–716 (1989).
13. C. K. Hong, Z. Y. Ou, and L. Mandel, "Measurement of subpicosecond time intervals between two photons by interference," *Phys. Rev. Lett.* **59**, 2044–2046 (1987).
14. M. Halder, S. Tanzilli, H. de Riedmatten, A. Beveratos, H. Zbinden, and N. Gisin, "Photon-bunching measurement after two 25-km-long optical fibers," *Phys. Rev. A* **71**, 042335-1–5 (2005).

1. Introduction

Since several years, photon pairs have become an important resource for quantum communication [1, 2, 3, 4]. Lately, effort has been concentrated on generating those pairs in waveguiding structures to increase efficiency and avoid collection and insertion losses. For instance, photon pair sources based on parametric fluorescence in periodically poled lithium niobate waveguides [5] or on four-wave mixing in silica fibers [6, 7] have been extensively studied. In 1999, G. Bonfrate *et al.* reported the observation of quasi-phase matched parametric fluorescence in a periodically poled D-shape silica fiber [8]. This suggested another promising photon pair source based on second-order nonlinearity in fibers. However, since that first demonstration, no further results have been reported.

In this paper, we report the observation of quasi-phase matched parametric fluorescence in periodically poled twin-hole silica fiber (PPSF). We also show that the measured signal arises from photon pairs by performing coincidence measurements and a Hong-Ou-Mandel experiment. Compared with the periodically poled D-shape fibers used in [8], twin-hole fibers have several advantages: they can be directly spliced to optical fibers so that the photon pairs are readily collected. Moreover, the technology for periodic poling in twin-hole fibers is compatible with tens of centimetres of interaction lengths, thus enabling higher conversion efficiency than in D-shape fibers. Finally longer interaction length also induces narrower spectral width of the created photon pairs which makes quantum communication schemes easier to implement.

2. Periodically poled twin-hole silica fiber

Since silica glass presents a vanishing second-order nonlinearity owing to its centro-symmetric structure on a macroscopic scale, the technique of thermal poling has been applied to twin-hole glass optical fibers in order to induce a permanent $\chi^{(2)}$, thereby enabling parametric second-order non-linear optical processes [10]. The twin-hole fiber owes its name to a pair of holes running parallel to the core along the fiber length (inset in Fig. 2). During the poling process a high voltage (~ 4 kV) is applied across the core thanks to two thin 25 μm -diameter wire electrodes that are inserted into the holes. Simultaneously the fiber is heated to 250 $^\circ\text{C}$. Under the action of the applied electric field, impurities ions, typically Na^+ , drifts away from the anode

leaving behind a negatively charged region. Sudden cool down of the glass freezes the ions in their new position and an intense electric field ($\sim \text{kV}/\mu\text{m}$) is consequently frozen in the glass. This electric field couples with the existing third-order nonlinearity to give an effective $\chi^{(2)}$ through the relationship $\chi^{(2)} = 3\chi^{(3)}E_{\text{dc}}$, where E_{dc} is the frozen field induced by poling. The poling time (10 min), voltage and temperature were chosen in order to maximize the overlap between the frozen-in field and the core of the fiber. A 8 cm long uniform $\chi^{(2)}$ nonlinear region was produced in this way. Quasi-phase matching for efficient growth of the parametric fluorescence power was implemented by periodic UV erasure of the uniform frozen-in field as described in [9].

The twin-hole fiber we used has a slightly elliptical core of diameter $3 \times 3.3 \mu\text{m}$, a numerical aperture of 0.27 ± 0.01 and a hole to core separation of $1.7 \mu\text{m}$. The 8 cm long poled region was spliced to SMF-28 fibers at both ends. However in this sample, the mode matching of the twin-hole fiber and the single mode fibers was not optimized, leading to significant splice losses ($\sim 3 \text{ dB/splice}$). This prevents us from knowing exactly how much pump power we inject in the fundamental mode of the poled fiber. This same sample has previously been used for demonstration of second-harmonic generation in a low-power all-fiber configuration[11]. The second-harmonic generation (SHG) wavelength tuning profile of the fiber is depicted in Fig. 1.

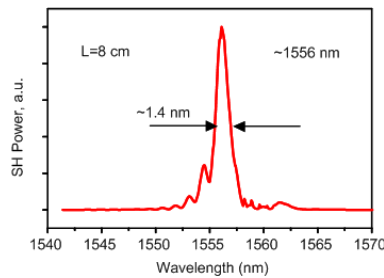


Fig. 1. Second-harmonic power (after removal of the pump) versus pump wavelength. The pump peak power is 220 W and the resonance is at 1556 nm. The acceptance bandwidth of the fiber is $\sim 1.4 \text{ nm}$ FWHM.

3. Coincidence measurement

The experimental setup for studying parametric fluorescence is described in Fig. 2. It consists of cw Ti-Sa laser tunable around 775 nm. The polarization of the pump beam is adjusted using a polarizing beam splitter (PBS) and a half-wave plate (HWP). The pump is injected in the fiber through a $\times 20$ microscope objective. Finally, at the output of the fiber, the pump is removed by dielectric long-wave pass filters (LWP) and the signal sent to a 3 dB coupler where the photon pairs are probabilistically separated. Each coupler output leads to an InGaAs/InP avalanche photodiode operating as single photon detector (ID Quantique id200). The Peltier cooled InGaAs/InP avalanche photodiodes (APD) are operated in gated mode (100 ns gate), at 10 kHz rate with a 10 % efficiency and a dark count probability of 10^{-5} per ns.

By carefully scanning the wavelength and the polarization of the pump field, we have found the poling resonance to be at 778 nm, leading to the generation of a degenerate signal field centered on 1556 nm in the fiber-optic communication band (Fig. 3(a)). This is consistent with the second-harmonic generation (SHG) measurements in this same poled fiber, see [11] and Fig. 1. At the maximum gain, the signal power before the 3 dB coupler can be obtained from the photon count rate (1.5 %). Taking into account the duty cycle ($\times 0.1 \text{ ms}/100\text{ns} = \times 10^3$), the 10 kHz rate, the dark counts, and the efficiency of the detector, the optical power detected by

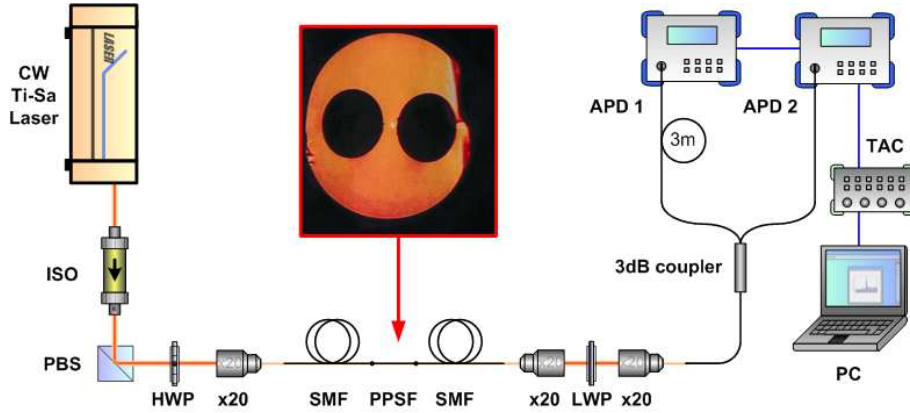


Fig. 2. Experimental setup: ISO, isolator; PBS, polarizing beam splitter; HWP, half-wave plate; X20, microscope objective; SMF, single mode fiber; PPSF, periodically poled silica fiber; LWP, long-wave pass filter; APD, avalanche photodiode; TAC, time to amplitude converter; Inset: Cross section image of the twin-hole fiber used in the experiment. Distance between the holes is 10 μm .

the APD is $P_o = 0.1$ pW. The pump power at the output of the single mode fiber was 43 mW which is 7 times smaller than the value reported in [8].

Theoretically, at degeneracy and in the low gain condition, the signal power can be approximated by

$$P_{\text{signal}} \approx \frac{\hbar\omega_s}{2\pi} B_\omega \eta_{SH} P_{\text{pump}}, \quad (1)$$

where η_{SH} is the second-harmonic generation efficiency normalized to the pump power and B_ω is the FWHM of the signal spectrum in rad/s. At degeneracy, the latter reads

$$B_\omega = \sqrt{\frac{2\pi}{\left. \frac{d^2\beta_s}{d\omega_s^2} \right|_{\omega_{s0}}} L}, \quad (2)$$

where β_s is the signal propagation constant, ω_{s0} the signal angular frequency at degeneracy and L the length of the poled section.

The dispersion $\left. \frac{d^2\beta_s}{d\omega_s^2} \right|_{\omega_{s0}}$ has been estimated using the method described in [12] based on white light interferometry, leading to a signal spectral width of 17 THz. This bandwidth is far bigger than the SHG bandwidth since parametric fluorescence may generate non-identical pairs of photons. As a result, the two generated photons may have different wavelengths as long as the total energy still adds up to 778 nm photon. Such a wide bandwidth can be problematic for quantum communication experiments. The standard method to overcome this problem is to use bandpass filters, see for instance [14]. In our experiment, the long-wave pass filter and the APD cut-off wavelengths reduce the effective bandwidth to 10.6 THz.

The second-harmonic efficiency η_{SH} has been measured to be 0.02 %/W. According to Eq. 1, and assuming a pump power of 43 mW, this leads to a predicted fluorescence power (signal+idler) of 37.4 pW at the output of the poled section. This theoretical result corresponds to a photon pairs rate of 146.2 MHz for the 17 THz bandwidth. However, the losses induced from the splices (not optimized) and the pump filtration setup have been estimated to be -9.8 dB. Taking into account the detector specifications (bandwidth, efficiency, gate...), it leads to a predicted

output power of $P_o^{th} = 3.92$ pW. This is quite far from the parametric fluorescence measured value ($P_o = 0.1$ pW). The discrepancy (-15.9 dB) on the signal power is attributed to the imprecision on the estimation of the splice losses and the amount of the pump power which is injected in the fundamental mode of the poled fiber. Indeed, the phase matching is only achieved for the fundamental mode. Coupling the pump power into this mode is difficult because the SMF-28 fiber, spliced at the ends of the PPSF, is multimode at this wavelength. Therefore, even slight bends can cause higher order modes to be excited resulting into significant changes in the value of P_o .

Finally, using Eq. 1, we estimated the conversion efficiency P_{signal}/P_{pump} at the output of the poled section. Since $P_o(\text{signal} + \text{idler}) = 0.1$ pW and since the losses induced by the filtering process are estimated to be 9.8 dB, we deduce $P_{signal} = 0.5$ pW. As a result, we deduced a conversion efficiency P_{signal}/P_{pump} of $1.2 \cdot 10^{-11}$ which is comparable to the value $6.4 \cdot 10^{-11}$ reported in [8] where they manage to efficiently inject in the fundamental mode. On the other hand if all the pump power was injected into the fundamental mode, we estimate that the conversion efficiency should be approximately $4 \cdot 10^{-10}$.

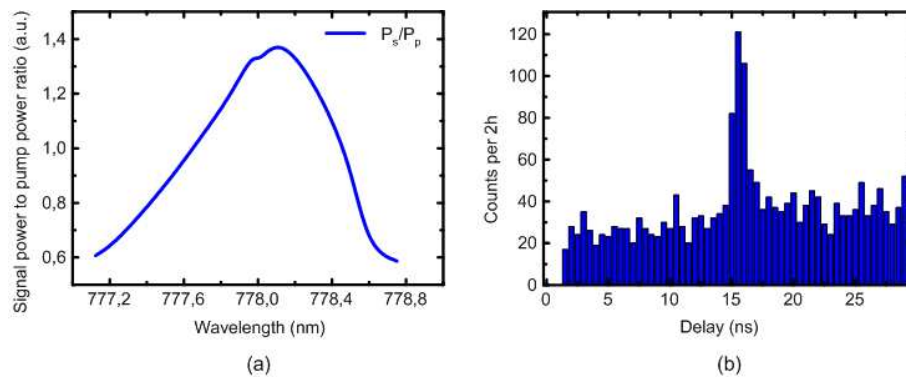


Fig. 3. (a). Parametric fluorescence power (after removal of the pump) to pump power ratio versus pump wavelength. The periodic poling resonance lies at 778 nm. (b) Coincidence histogram: each slot is 0.5 ns long. The peak in the histogram is a signature for time-correlated photons. It shows a SNR of 4. The pump power measured at the output is 43 mW.

As regards the coincidence measurement, a time to amplitude converter (TAC) allowed us to plot the delay between the detection times of the two APD's (Fig. 2). In the setup, we added a 3 m fiber delay line in front of one of the APD's, corresponding to a 15 ns delay between photon arrival times at the detectors. Thus, the presence of a peak at 15 ns in the histogram is a signature for time-correlated photons created by parametric fluorescence in the poled fiber. A signal to noise ratio (SNR) of 4 is obtained (Fig. 3(b)) with 43 mW pump power. It improves the 1.5 SNR reported in [8]. A coincidence count rate of 255 counts per two hours over 3 ns (6 slots) is measured thanks to the TAC. It means a 0.035 Hz coincidence rate that is related to a 3.5 kHz effective photon pair rate arriving on the APDs. This value has to be compared to a theoretical expected value of 342 kHz that results from the 146.2 MHz theoretical photon pair rate mentioned above, decreased by losses (-26.3 dB) resulting from splice and filters (-9.8 dB \times 2), coupler (-3 dB since a photon pair has 50% chance to be splitted), bandwidth limitation (-2 dB for filters and APDs and -1 dB for the coupler), and connectors (-0.12 dB \times 3 \times 2). If we also include the pump coupling efficiency (-15.9 dB) calculated from the previous measurement, the expected rate of 8.8 kHz is in good agreement with the 3.5 kHz measured rate.

To conclude, this result could still be significantly improved by optimizing the coupling of

the pump to the fundamental mode -which could be achieved by removing the SMF-28 pigtail at the input-, and by reducing the splice losses between the poled section and the single mode output fiber. The latter improvement can be achieved using a high N.A., small core fiber instead of the SMF-28, or by putting a buffer fiber with intermediate core size between the PPSF and the SMF-28, or by inducing a taper between both fibers. In recent work, we have reduced the splice loss to ~ 1 dB. Moreover, an all-fiber set-up to remove the pump and more efficient detectors may also be used. Recent experiments with an all-fiber filtration set-up reduced the -9.8 dB losses to -2.8 dB.

4. Hong-Ou-Mandel experiment

In order to validate this photon-pair source, a Hong-Ou-Mandel experiment[13] was realised using an all-fiber Michelson interferometer. As shown in the schematic description Fig. 4(a), photon pairs enter the interferometer via an optical circulator. The circulator sends the photon

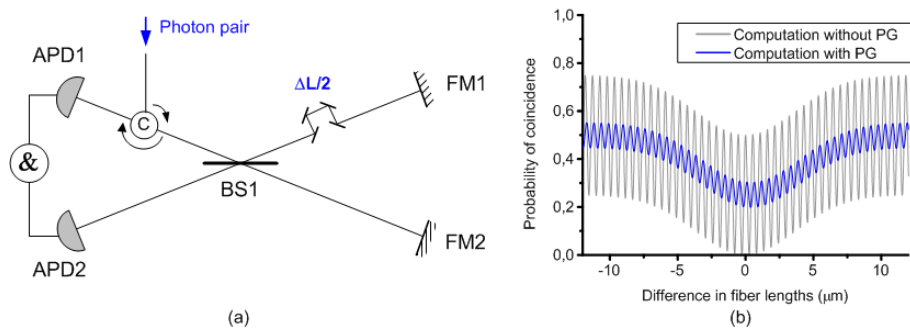


Fig. 4. (a). Schematic depiction of the experimental set-up for observing the Hong-Ou-Mandel dip. Photon pairs may be splitted on a 50/50 beam-splitter (BS1) and recombined on the same beam-splitter after reflection on two Faraday mirrors (FM1 and FM2). The coincidence rate between the two outputs is measured as a function of the delay ΔL set on the upper arm. (In the actual experiment, optical-fiber components are used) (b) Theoretical coincidence probability versus the delay ΔL : expected two-photons interferences prevent the dip to be easily observed (gray line). Small variations over ΔL can be induced by a pattern generator (PG) to lower this effect (blue line).

pairs on a 50/50 beam-splitter (BS1) (in practice a 3dB fiber coupler) where they can be separated. The photons then propagate towards Faraday mirrors placed at the end of each arm of the interferometer (going from left to right in Fig. 4(a)). After reflection, they come back to the beam-splitter (BS1) (going right to left). One arm is slightly longer, and introduces a total extra optical path ΔL . If ΔL is set to zero the two photons that come back to the beam-splitter are indistinguishable, and they experience photon bunching[13]. As in the original Hong-Ou-Mandel experiment, detectors are put at the beam-splitter outputs, and the number of coincidences is measured as a function of the delay ΔL . One expects a substantial dip in the coincidence rate when $\Delta L = 0$. In our case, twin photons only have 50 % chance to be separated when they first go through the beam-splitter (left to right). As a result, both single-photon and two-photon interferences occur when they come back to the beam-splitter (right to left). As discussed by Halder *et al.*[14], the coincidence probability that results from the superposition of the two phenomena is

$$P_c \propto 2 - e^{-\Delta\omega^2\tau^2} - \cos \omega_p \tau, \quad (3)$$

where $\Delta\omega$ is the fluorescence bandwidth (approximated to be Gaussian), τ is the time delay induced by the optical path difference ΔL and ω_p is the pump pulsation. When plotted against

τ , the $e^{-\Delta\omega^2\tau^2}$ term results in a dip that is the Hong-Ou-Mandel signature. In the Fig. 4(b), the expected coincidence probability is plotted with respect of ΔL (gray curve). One sees the one-photon interference fringes superposed on the dip. The interfringe spacing is related of the pump wavelength, whereas the dip for a 10.6 THz bandwidth is expected to be $7.3 \mu\text{m}$ wide. In our experiment the fiber in each arm was individually temperature controlled thanks to two Peltier modules powered by PID temperature controllers. Thus ΔL could be tuned using the fiber thermal expansion. The fiber length difference between the two arms of the interferometer is first measured using white-light interferometry. As illustrated by Fig. 5(a), a temperature difference close to 10°C is set in order to cancel the length difference between the two arms. Similarly to Sec 3, APD's are used in order to perform coincidence measurements for different ΔL values.

In our experiment we observed peaks and dips in the coincidence rate and in the power measured by the two APD's, corresponding to the interference fringes predicted by Eq. 3. However the stability of the interferometer was not sufficient to reliably measure these interference fringes over a long period. The resulting noisy data would have masked the presence of the Hong-Ou-Mandel dip, which was the main aim of the experiment. To solve this problem we periodically induced a small variation on the delay ΔL that with an amplitude of approximately $\lambda/2$. As a result the fringes are averaged during acquisition time as illustrated by the blue curve in Fig. 4(a). This slight variation was achieved thanks to a $\pm 0.01^\circ\text{C}$ temperature variation of one arm induced every 30 s by a pattern generator. With this averaging the coincidence rate shows a clear $8.4 \mu\text{m}$ dip as shown in Fig. 5(b). As a consequence of the averaging the dip is slightly broader than the expected value from Eq. 3 ($7.3 \mu\text{m}$). When the noise is subtracted, the net visibility is 40%. In the Fig. 5(b), the measurements are compared to theory and show good agreement.

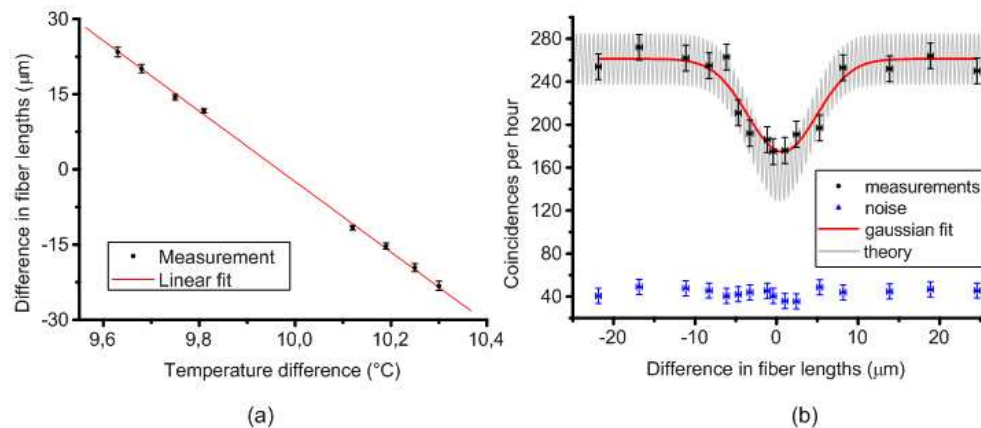


Fig. 5. (a) Differences in fiber lengths measured by white-light interferometry versus temperature difference between the two arms of the interferometer. (b) Coincidence measurements at the Michelson interferometer outputs (black dot) for 45 mW pump power measured at the output of the PPSF and gaussian fit (red curve); The coincidence rate is calculated over 3 ns time window (4 slots); the error on the coincidence number is due to the dark counts; the horizontal error is due to the slight modulation of ΔL ; the blue points show the accidental events. The theoretical curve (grey) takes into account the spectral width of the produced photon pairs, and the slight modulation of ΔL . It has a 50% maximum visibility (after accidental events are subtracted). Note that we have a higher coincidence rate than in section 3 thanks to a better coupling of the pump to the fundamental mode

5. Conclusion

In conclusion, we showed that with lower pump power than in [8] we were able to observe parametric fluorescence in a periodically poled silica fiber and measure a coincidence peak with a SNR of 4. This source is highly broadband with 17 THz theoretical bandwidth. The poled region was spliced to standard single mode fibers which shows that the source could be easily integrated in fiber-optic communication systems. A Hong-Ou-Mandel dip with 40% net visibility has been observed. It demonstrates that periodically poled twin-hole silica fibers are valid candidates as sources for quantum communication. Finally, today, we have manufactured poled fibers up to 25 cm long and nonlinearities up to four times the one induced here. This suggests that further improvements on photon pair source based on parametric fluorescence in periodically poled twin-hole silica fiber can be expected.

Acknowledgments

The authors thank Freddy Clavie for his precious technical help and constant support. The authors also acknowledge the support of the Fonds pour la formation à la Recherche dans l'Industrie et dans l'Agriculture (FRIA, Belgium), of the Interuniversity Attraction Pole program of the Belgian government under Grant IAP6-10 and of the EU project QAP contact number 015848.

*Present address, Solid State Physics Lab., Facultés Universitaires Notre-Dame de la Paix, Rue de Bruxelles 61, B-5000 Namur, Belgium.